Assessing the Impact of Twisting and Bending Deformations on Flexible Interconnect Performance

Ekrem Altinozen, *Graduate Student Member, IEEE*, Ana Vukovic, *Member, IEEE*, Phillip Sewell

***Abstract*—Flexible interconnects are essential components for signal transmission for foldable and wearable electronics. As such they are exposed to a variety of mechanical deformations that can degrade their electromagnetic performance. This paper analyses the impact of bending and twisting deformations on the transmission properties of a variety of commercially available polymer and elastomer based interconnects and compares to the performance of flat interconnects fabricated on rigid substrates. The analysis of the impact of deformations also takes into account the degradation in the conductivity of the printed lines due to reported mechanical deformations.**

***Index Terms*—computational electromagnetics, fully flexible interconnect, space deformation techniques, Green Coordinates**

I. INTRODUCTION

Wearable electronic devices are a rapidly expanding area for a range of applications from sport to biomedicine. Flexible interconnects are essential components for signal transmission and a large volume of research has been focused on novel dielectric and conductive materials that can effectively withstand the deformations these components are exposed to. E-textile, woven and knitted textile structures are inherently flexible but suffer from implementation uncertainty in large-scale production [1, 2]. The most popular dielectric materials are those made from *polymers* such as polyethylene terephthalate, (PET) , and polyimide (PI) [3-5], and *elastomers* such as polydimethylsiloxane (PDMS) and polyurethane (PU) [6-8]. The electrical properties, dielectric constant and loss tangent for the operating range 1-10 GHz and key mechanical properties of PET, PI, PDMS, and PU substrates are summarized in Table I. According to the mechanical properties in Table I [9], (density, Young modulus and elongation), elastomers (PDMS and PU) provide higher deformability compared to polymers (PET and PI) substrates, however polymers offer higher electrical and thermal stability in practical environmental conditions. It can also be seen that the PU material has the highest dielectric losses whilst the PI material has the lowest dielectric losses.

TABLE I
TYPICAL PHYSICAL PROPERTIES OF POLYMER AND ELASTOMER SUBSTRATES FOR INTERCONNECTS

Properties	PI	PET	PDMS	PU
Density (g cm^{-3})	1.42	1.39	0.95-0.98	1.0-1.30
Young's modulus (GPa)	2.5	5	<0.01	<0.01
Ultimate Elongation (%)	80	90	50-500	300-800
ε_r 1 GHz–10 GHz	3.4–3.5	3.0	2.75-2.9	2.14-3.5
$tan\delta$ at 1GHz–10 GHz	0.0020–0.0027	0.002-0.008	0.008–0.07	0.02-0.1
Deformability	Low	Low	High	High
Thermal Stability	High	High	Low	Low
Electrical Stability	High	High	Low	Low
Fabrication	Simple	Moderate	Moderate	Moderate

Note: Young's modulus. Data taken from [9] (The range for flat substrate is for the frequencies range 1-10 GHz).

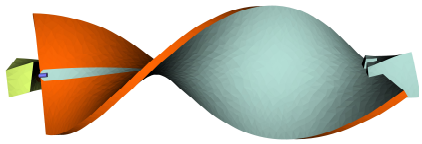

Fig. 1. An example of extreme twisting of a flexible interconnect.

A wide range of novel electrically conductive materials that are compatible with polymer and elastomer based substrates have been reported, namely nanowires (NW) [10], graphene [11], Ag stretchable conductors [7], liquid metals [12], conductive polymers [6, 8] and conductive fibres [13]. However, their typical conductivity depends on the particle and ink composition and is typically poorer than that of traditional rigid metals [4, 5]. Additionally, the methodology of depositing metallic traces influences their thickness which can range from 15-25μm for screen printed metal flake polymer compounds [4, 14], to 1-3μm for inject printed traces [5], and 0.20 mm for

This paragraph of the first footnote will contain the date on which you submitted your paper for review. It will also contain support information, including sponsor and financial support acknowledgment. For example, "This work was supported in part by the U.S. Department of Commerce under Grant BS123456".

The next few paragraphs should contain the authors' current affiliations, including current address and e-mail. For example, F. A. Author is with the National Institute of Standards and Technology, Boulder, CO 80305 USA (e-mail: author@ boulder.nist.gov).

S. B. Author, Jr., was with Rice University, Houston, TX 77005 USA. He is now with the Department of Physics, Colorado State University, Fort Collins, CO 80523 USA (e-mail: author@lamar.colostate.edu).

T. C. Author is with the Electrical Engineering Department, University of Colorado, Boulder, CO 80309 USA, on leave from the National Research Institute for Metals, Tsukuba, Japan (e-mail: author@nrim.go.jp).

filament printing [15]. The thickness of the signal trace also limits the inherent flexibility of the components [9]. The limited structural stability of conductive prints under deformations [14] is typified by the appearance of nano and micro gaps that cause loss of current continuity [4, 6, 7, 14, 16].

Our earlier study of flat flexible interconnects showed that interconnects fabricated on PET and PI substrates have the smallest transmission losses compared to PDMS and PU substrates and that interconnects fabricated on PU substrates have the highest losses [17]. The losses are predominantly due to increased substrate losses as shown in Table I.

Flexible interconnects also need to effectively withstand a wide range of complex deformations such as, for example, crumpling, bending, wrinkling and twisting. An example of extreme twisting deformation on a flexible interconnect is shown in Fig. 1. However, analysis of the impact of deformations on the performance of flexible interconnects is limited. Commercial simulation packages provide means for generating one-dimensional bending i.e., bending over a cylindrical plane. For this reason, the flexibility of RF interconnects is evaluated both experimentally and computationally for the case of simple cylindrical bending [4, 11, 18], and for more complicated 2D deformations, such as twisting, only experimental results for the interconnects on the PI and textile substrates are available [5]. Furthermore, these limited experimental and computational results have been reported for interconnects fabricated on PDMS [8], and PI [5], each under different conditions so that comparative evaluation across a comparable range of components is difficult to make.

In this paper we extend the analysis to evaluate the impact of bending and twisting on the performance of a variety of realistic interconnects designed for commercially available polymer and elastomer substrates. The EM performance of interconnects under deformation and fabricated on a range of substrates, namely PI, PDMS, PU and PET, is systematically analyzed and compared to interconnects designed on a rigid substrate with the aim of ascertaining the most resilient platform for flexible electronics. All interconnects are assumed to have realistic dielectric and metallic losses.

Computational geometrical models of cylindrical deformation are made using standard Boolean CAD approach based on constructive solid geometry (CSG). However, this CAD approach is not reliable for generating twisting deformation as it may result in formation of microscopic gaps between constitutive layers of the interconnect (ie, substrate/ground plane/metallic trace) which can undermine electromagnetic simulations, as discussed in [19]. To overcome this difficulty we apply a computer graphics approach based on Green Coordinate (GC) technique for spatial manipulation of objects to create desired twisting deformation [20, 21]. The full description of how GC methodology is implemented for the purposed of electromagnetic (EM) simulations is discussed in detail in[17, 19].

To characterize the EM performance of the interconnects, we use an in-house three-dimensional (3D) numerical time-domain Transmission Line Modelling (TLM) method [22] based on unstructured tetrahedral Delaunay mesh [23-26]. The unstructured mesh variant of the TLM algorithm is second-order accurate with respect to the wavelength [25]. Compared to similar time-domain EM solvers, like Finite Difference Time Domain (FDTD), [27], the main advantage of the unstructured TLM method is that all field components are co-located in space and time and stability is provable on a cell-by-cell basis without invoking the Courant condition. The unstructured TLM method has been industrially characterized for a range of applications including EMC [28, 29], aerospace [30,31] and full details on unstructured TLM methodology is available in [23-26].

The paper is structured as follows: Section II summarizes the computational models of interconnects designed for PET, PDMS, PI, and PU substrates. Section III analyses the impact of convex and concave bending on a variety of realistic interconnects and compares it to the performance of the flat rigid interconnect. Section IV analyses the impact of twisting on EM performance of a variety of interconnects. In both cases the conductive losses with and without the impact of deformation are considered. Section V summarizes the main conclusion of the paper.

II. Computational Models

This section summarizes the design parameters of a range of interconnects designed for commercially available substrates, namely Sylgard 184 (PDMS) [6], Ninja-Flex (PU) [15], Kapton (PI) [5], Melinex (PET) [4], and RO4350 [30]. The substrate thickness of PI and PET substrates is taken to be 0.2mm in accordance with [5]. The thicknesses for PDMS and PU substrates is considered to be 1 mm [6]. A realistic measurement setup is considered where interconnects are connected to the 50 Ω coaxial cable via a standard sub-miniature A (SMA) connector.

In order to minimize reflections at the cable-interconnect interfaces all interconnects are designed to have 50 Ω characteristic impedance. This implies that different substrate thicknesses will dictate the width and length of the signal trace according to microstrip line synthesis equations [31].

TABLE II
Design Parameters

Thickness [mm]	W_{PI} [mm]	W_{PDMS} [mm]	W_{PET} [mm]	W_{PU} [mm]	ri	ro
0.200	0.500	-	0.507	-	0.254	0.822
1.0	-	2.50	-	2.79	0.635	2.055
	PI [5]	PDMS [6]	PET [4]	PU [15]		
ε_r	3.1	2.77	3.0	2.60		
tan (δ)	0.007	0.01	0.002	0.07		
σ [S/m]	1×10^6 [5]	3.33×10^5 [7]	5×10^5 [4]	1.6×10^4 [15]		
Track Thickness	3 µm	140 µm	20 µm	200 µm		

Note: Design parameters for PI and PET interconnects are given for two different cases of substrate thicknesses.

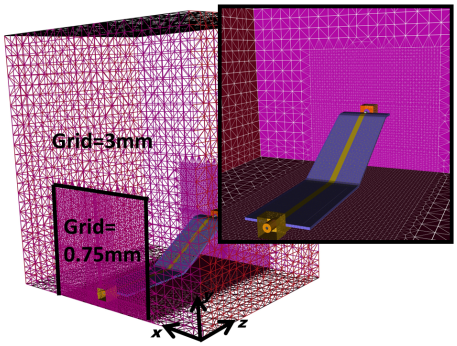

(a)

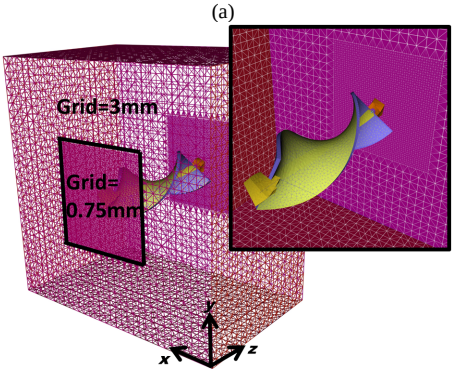

(b)

Fig. 2. Meshed computational domain of the interconnect with a) bending and b) twisting deformation.

Table II summarizes the widths (W) of the signal traces, and typical dielectric constant, ε_r, dielectric loss, tanδ, for PI, PDMS, PET, and PU interconnects. The typical conductivity, σ, of metallic prints commonly fabricated on respective substrates is also given in Table II. For all cases, the coaxial cable has an impedance of 50 Ω with relative permittivity, ε_r=2. The inner, r_i, and outer radius, r_o, of the coaxial cables for relevant substrate thicknesses are also summarized in Table II.

Unstructured tetrahedral meshing is ideally suited to sampling a problem that does not align to a cartesian coordinate system. A three-dimensional (3D) Delaunay Mesher [24, 25, 32] is used to discretise the problem space. For the case of the flat and bent interconnects the overall computational domain is set to be $1.21\lambda \times 0.94\lambda \times 1.21\lambda$ where λ is the free space wavelength at 5 GHz. For the case of the bent and twisted interconnects the overall computational domain is set to be $1.67\lambda \times 1.03\lambda \times 1.67\lambda$. Note that in the case of the flat interconnect the region under the interconnects' ground plane is reduced to optimise the computational resources without affecting the accuracy of the results. The meshed computational domain of the bent and twisted interconnects is given in Fig.2(a,b) where it can be seen that the discretisation deploys a hybrid mesh that combines a cubic mesh around uniform regions and a tetrahedral mesh around the curved regions.

The near field of the interconnect is meshed with cubic cells of 0.75 mm (for 1 mm substrates) or 0.375 mm size (for thinner substrates) and a bigger mesh of 3 mm cubic cell size is used for the region further away from the interconnect. The computational domain is truncated with free space impedance boundary conditions.

To efficiently manage computational resources, the printed signal line and ground plane are not directly meshed but are

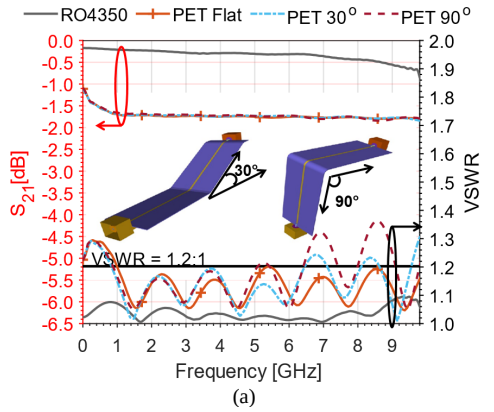

(a)

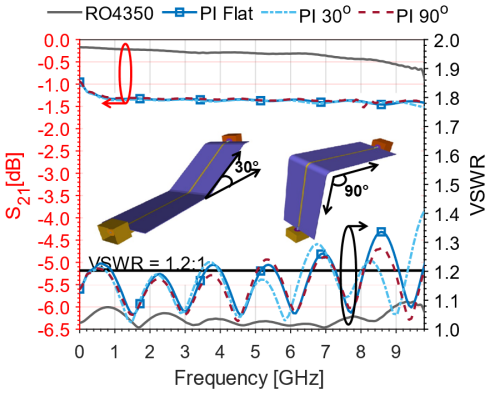

(b)

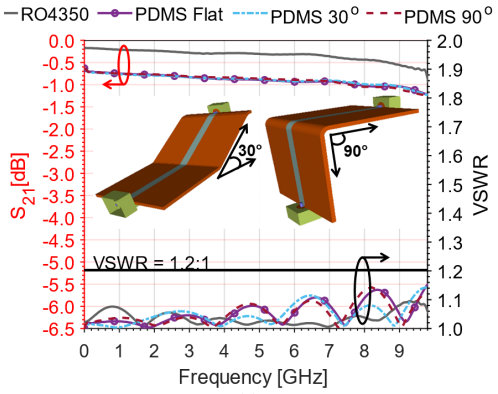

(c)

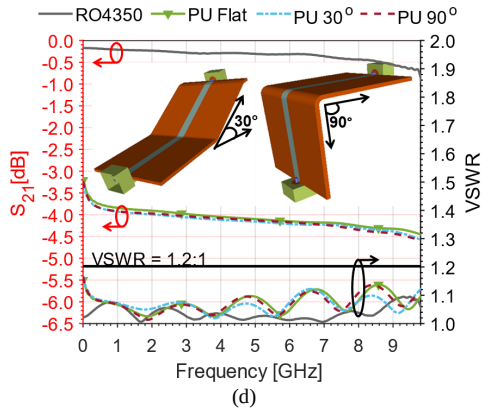

(d)

Fig. 3. Comparison of S_{21} and VSWR for flat and 30° and 90° degree bent interconnects designed on a) PET substrate, b) PI substrate, c) PDMS and d) PU substrate. For reference transmission properties of a flat interconnect designed on a rigid substrate is also given. Metallic losses are considered.

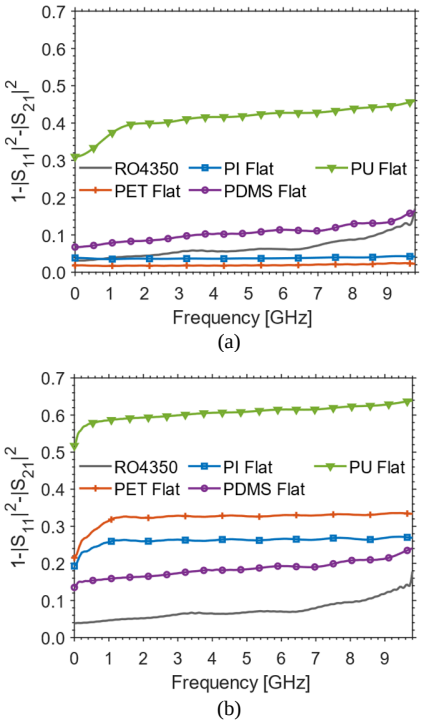

Fig. 4 Total loss of flat flexible interconnects and rigid transmission line with (a) only dielectric losses included and (b) both dielectric and conductive losses included.

embedded between computational cells as outlined in [26]. One-dimensional (1D) analytic transmission line models are used to characterise the lossy conductive layer as described in [26].

In all simulations the interconnect is excited with the fundamental TEM mode of the coaxial cable with a spectrum from 0.25 GHz to 10.25 GHz. For all simulations the timestep taken is 6.67128 ns and simulations are run for 3 million timesteps.

III. Performance Under Bending Deformations

This section investigates the impact of bending on the transmission properties of interconnects for a range of commercially available flexible substrates.

Fig. 3(a-d) compares the impact of 30° concave and 90° convex bending deformation on the 50 Ω interconnect designed on a) PET substrate, b) PI substrate c) PDMS substrate and d) PU substrate. All substrates are 12.7 mm wide and 50 mm long. In all cases their performance is compared to the flat flexible interconnect and also against a conventional flat interconnect designed for the rigid substrate RO4350 (substrate thickness= 1 mm, ε_r=3.48, tanδ = 0.0037, σ=4.41× 10^7 S/m, metallic line thickness of 2.287 mm). Results for all interconnects assume substrate and conductive losses as given in Table II.

According to Fig. 3(a,b) for thin substrates, the PET and PI based interconnects exhibit similar performance with transmission losses of around 1.5dB-2 dB over the operating band. The results for PET interconnect agree very well with experimental measurements for a 30° bend reported in [4]. The PU based interconnects have the highest losses compared to PET, PI and PDMS based interconnects. Fig.4 shows that the PDMS based interconnect has the overall best performance in terms of transmission loss. In all cases, concave or convex bending does not significantly affect the transmission properties. However, when compared to the conventional rigid interconnect the flexible interconnects are overall more lossy. This can be explained by the fact that flexible substrates and conductive material have higher material losses (tanδ) and conductive losses (σ) compared to conventional gold microstrip line on a rigid substrate.

To separate dielectric and conductive losses, Fig. 4(a,b) compares the total system losses of flat interconnects for the case where a) only dielectric losses of transmission lines are considered and b) both dielectric and conductive losses are considered. Fig.4 shows that in the absence of metallic losses the best performing are PET and PI interconnects that are outperforming the conventional rigid microstrip line. The PU based interconnect has the highest dielectric losses. Fig.4b) shows that when metallic losses are added all flexible interconnects have increased system losses which is as expected. In the absence of metallic losses the rigid transmission line has the lowest losses which is primarily due to the low conductive losses of the metallic line. PDMS based interconnects have the smallest system losses, PI and PET based interconnects have similar losses whilst the PU based interconnect remains the most lossy transmission system. Comparing the losses values from Table II, it can be seen that PI based interconnect has smaller dielectric and conductive loss compared to PDMS line but higher overall loss. This can be explained by the fact that the width of the PI line is much smaller compared to the PDMS line meaning that field is less concentrated in the substrate and implying that the additional loss of the PI line is due to radiation losses.

IV. Performance Under Twisting Deformations

In this section the impact of twisting deformation on a range of interconnects is analyzed.

Fig. 5 explores the impact of twisting deformation for two different lengths of the PDMS interconnect, namely a) 50 mm and b) 25 mm. The substrate width is 12.7 mm. All other parameters of the interconnects and coaxial lines are given in Table II. Metallic losses are neglected. The inset of Fig.5 shows the image of the interconnect under twisting deformation. The twisting is characterized by an angle ρ and is perfomed in anticlockwise direction, as shown in Fig. 5.

Four different twisting deformations are considered namely, ρ=22.5°, 45°, 58.5° and 96°. Fig. 5(a) shows the results for 50 mm long PDMS and Fig.5(b) for 25 mm long PDMS interconnect. Results for the flat PDMS are also included for reference. The S_{21} parameter is unaffected by the twisting angle at lower frequencies whilst the number of peaks in VSWR depends on the length of the interconnect and the main operating wavelength. This implies that the reflections are caused by the combination of deformation that affects the impedance mismatch between the mode propagating along the interconnect and the coaxial line. The results for the flat case set a level for the connector mismatch. The fact that peaks are not at the same level illustrates that there exists radiative coupling to the connector in addition to the fundamental mode

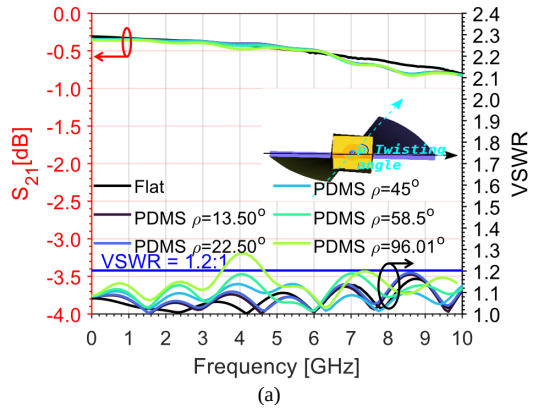

(a)

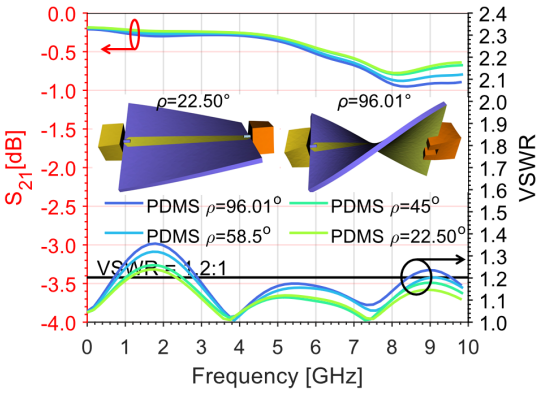

(b)

Fig. 5. S_{21} and VSWR for interconnects with twisting deformation designed for the PDMS substrate that is a) 50 mm long and b) 25 mm long. Twisting by angle of 22.50°, 45°, 58.5°, 96.01° is considered. The inset figure shows the rotation direction of twisting deformation. Metallic losses are neglected.

and this contributes to increased VSWR. As the waveguide is twisted the strength of the radiative coupling will vary.

Fig. 6 shows the impact of twisting deformation for the angle of 58.50° for PI and PET based interconnects fabricated on thin 0.2 μm subtrate and compares it to the perfomance of flat interconnects. All interconnects are 50 mm long and the realistic metallic and dielectric losses are assumed as given in Table II. The twisting deformation has similar impact on the transmission characteristic of PET and PI based interconnects and the VSWR can increase above desired value indicating increased reflection losses.

Printing or fabrication process of a conductive line on a flexible substrate may not be perfect and can result in microcracks or nano-holes in the conductive trace [5, 7, 14]. Repeated torsional deformation on such interconnects can result in the expansion of these non-uniform microcracks which in turn causes reduction in the overall conductivity of the conductive trace [5, 7, 14]. According to [14] when the interconnect is exposed to repeated twisting deformation conductivity of the metallic trace can be reduced by 33.33 % for PET and 16.66 % for PI interconnects respectively. To account for that Fig. 7 demonstrates the impact of reduced conductivity for the case of deformation angle of 58.50°.

Comparing the results of the flat and flexible PET and PI interconnect with degraded conductivity it can be seen the reduction in the conductivity has resulted in the increased

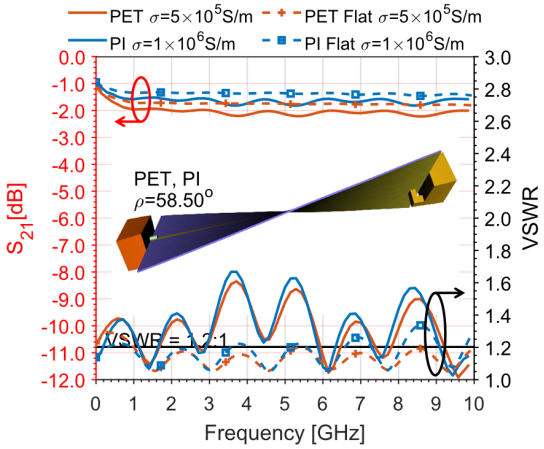

Fig. 6. Comparison of S_{21} and VSWR for the flat and twisted interconnect designed for the PET and PI substrate. Twisting angle is 58.50°, and realistic conductivity is assumed.

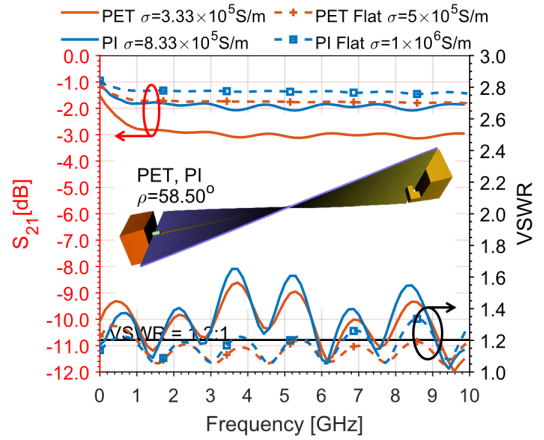

Fig. 7. Comparison of S_{21} and VSWR for the flat and twisted interconnect designed for the PET and PI substrate. Twisting angle is 265.17°, and the conductivity of metallic line for deformed case has changed according to [14] and given in the figure.

transmission loss in the range 0.5-1 dB over the operating band as well as increased VSWR. This is as expected considering the degraded conductivity effectively means a more lossy structure.

When it comes to thicker substrates, Fig. 8 demonstrates the return and insertion loss of PDMS, PU interconnects for the case of twisting deformation of 58.50°. This deformation does not significantly affect the line transmission performance and the results agree with experimental ones reported in [5]. The VSWR remains below desired 1.2 value.

Fig. 9 extend the analysis by taking into account the degradation of conductivity of the line under repeated deformation which, according to [14], results in conductivity being reduced by 33.33 % for both PDMS and PU interconnects. Again, it can be seen that the reduction in the conductivity has resulted in increased insertion loss of the interconnects by 0.5-1 dB over the operating band. The PDMS has overall the smallest transmission losses compared to other types of flexible interconnects.

Finally, Fig. 10 includes the impact of conductivity degradation for the case of extreme twisting deformation of 265.17° for the interconnects based on PDMS and PU substrate that have high elasticity. The change in conductivity is taken

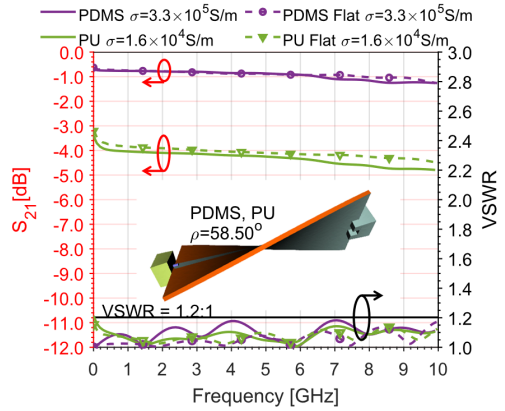

Fig. 8. Comparison of S_{21} and VSWR for the flat and twisted interconnect designed for the PDMS and PU substrate. The twisting angle is 58.50°, and realistic conductivity is assumed.

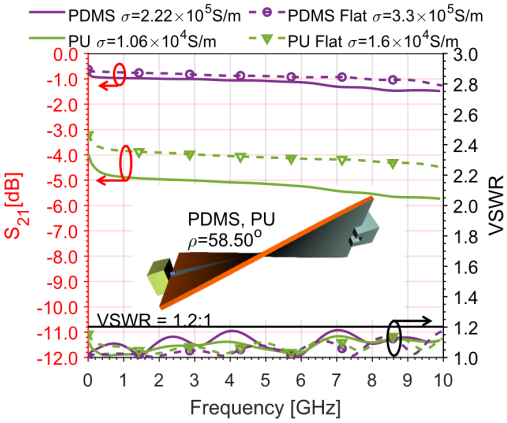

Fig. 9. Comparison of S_{21} and VSWR for the flat and twisted interconnect designed for the PDMS and PU substrate. Twisting angle is 58.50°, and the conductivity of metallic line for deformed case has changed according to [14] and given in the figure.

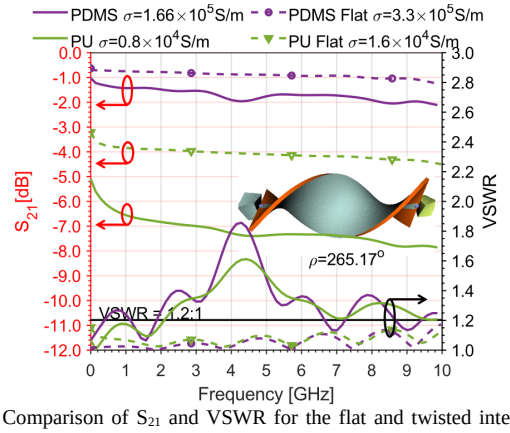

Fig. 10. Comparison of S_{21} and VSWR for the flat and twisted interconnect designed for the PDMS and PU substrate. Twisting angle is 265.17°, and the conductivity of metallic line for deformed case has changed according to [14] and given in the figure.

from [14] that predicts 50% reduction in conductivity for PDMS and PU substrates. Fig. 10 shows that PDMS based interconnects provide better transmission performance compared to interconnects based on PU substrates and provide a good solution where higher deformability is expected.

V. CONCLUSION

The rise of flexible electronics demands tools that can assess the impact of deformations. This paper presents a comprehensive analysis of the impact of twisting and bending deformation on the transmission properties of interconnects designed for the four most popular types of polymers and elastomer based flexible substrates namely, PET, PI, PDMS and PU substrates. The paper summarizes the electrical and mechanical properties of these substrates and typical conductivity achievable with modern fabrication technologies.

The paper analyses the impact of bending and twisting deformation in order to separate and independently quantify these two effects. In the case of bending, both concave and convex cases are considered. It is shown that the impact of bending deformation does not have significant impact on the line performance.

Twisting deformation has a small impact on the transmission loss at low frequencies [5] but the twisting deformation contributes to the radiative coupling to the connector causing worsening of the VSWR. The paper confirms that even when the impact of deformation on the metal conductivity is considered, the performance of PI [5], PDMS and PET interconnects remains stable [5]. For thin substrate PI provides better performance compared to PET substrates.

Interconnects based on PDMS substrates have mechanical properties similar to PU substrates, but due to overall lower substrate and conductive losses they are a better candidate for flexible electronics. The paper shows that interconnects based on PDMS exhibit the best performance even under extreme deformation making them suitable for applications that require high deformability.

REFERENCES

[1] K. Yan, J. Li, L. Pan, and Y. Shi, "Inkjet Printing for Flexible and Wearable Electronics," *APL Materials*, vol. 8, no. 12, p. 120705, 2020, doi: 10.1063/5.0031669.

[2] Y. Wu, S. S. Mechael, and T. B. Carmichael, "Wearable E-Textiles Using a Textile-Centric Design Approach," *Acc Chem Res*, vol. 54, no. 21, pp. 4051-4064, Nov 2 2021, doi: 10.1021/acs.accounts.1c00433.

[3] J. Wang, S. Lam, and E. G. Lim, "RF performance evaluation of microstrip lines printed on flexible polyethylene terephthalate (PET) films," in *2015 IEEE MTT-S International Microwave Workshop Series on Advanced Materials and Processes for RF and THz Applications (IMWS-AMP)*, 1-3 July 2015 2015, pp. 1-3, doi: 10.1109/IMWS-AMP.2015.7324924.

[4] Y. Shi, Z. Jiang, S. Lam, M. Leach, J. Wang, and E. G. Lim, "Multi-GHz Microstrip Transmission Lines Realised by Screen Printing on Flexible Substrates," presented at the 2017 IEEE Electrical Design of Advanced Packaging and Systems Symposium (EDAPS), 2017.

[5] S.-m. Sim, Y. Lee, H.-L. Kang, K.-Y. Shin, S.-H. Lee, and J.-M. Kim, "RF Performance of Ink-jet Printed Microstrip Lines on Rigid and Flexible Substrates," *Microelectronic Engineering*, vol. 168, pp. 82-88, 2017, doi: 10.1016/j.mee.2016.11.011.

[6] R. A. Liyakath, A. Takshi, and G. Mumcu, "Multilayer Stretchable Conductors on Polymer Substrates for Conformal and Reconfigurable Antennas," *IEEE Antennas and Wireless Propagation Letters*, vol. 12, pp. 603-606, 2013, doi: 10.1109/lawp.2013.2260123.

[7] D. Ding, R. Li, J. Yan, J. Liu, Y. Fang, and Y. Yu, "Influence of Microcracks on Silver/Polydimethylsiloxane-Based Flexible Microstrip Transmission Lines," *Applied Sciences*, vol. 11, no. 1, 2020, doi: 10.3390/app11010005.

[8] I. Cherukhin, S. P. Gao, and Y. X. Guo, "Fully Flexible Polymer-based Microwave Devices: Materials, Fabrication Technique, and Application to Transmission Lines," *IEEE Transactions on Antennas and Propagation*, pp. 1-1, 2021, doi: 10.1109/TAP.2021.3083855.

[9] D. Wang, Y. Zhang, X. Lu, Z. Ma, C. Xie, and Z. Zheng, "Chemical Formation of Soft Metal Electrodes for Flexible and Wearable Electronics," *Chem Soc Rev*, vol. 47, no. 12, pp. 4611-4641, Jun 18 2018, doi: 10.1039/c7cs00192d.

[10] S. Choi *et al.*, "Highly conductive, stretchable and biocompatible Ag-Au core-sheath nanowire composite for wearable and implantable bioelectronics," *Nat Nanotechnol*, vol. 13, no. 11, pp. 1048-1056, Nov 2018, doi: 10.1038/s41565-018-0226-8.

[11] X. Huang *et al.*, "Highly Flexible and Conductive Printed Graphene for Wireless Wearable Communications Applications," *Sci Rep*, vol. 5, p. 18298, Dec 17 2015, doi: 10.1038/srep18298.

[12] W. Chen, Y. Li, R. Li, A. V. Thean, and Y. Guo, "Bendable and Stretchable Microfluidic Liquid Metal-Based Filter," *IEEE Microwave and Wireless Components Letters*, vol. 28, no. 3, pp. 203-205, 2018, doi: 10.1109/LMWC.2018.2799382.

[13] Z. Wang, L. Zhang, Y. Bayram, and J. L. Volakis, "Embroidered Conductive Fibers on Polymer Composite for Conformal Antennas," *IEEE Transactions on Antennas and Propagation*, vol. 60, no. 9, pp. 4141-4147, 2012, doi: 10.1109/TAP.2012.2207055.

[14] R. Mukherjee, A. S. Dahiya, and R. Dahiya, "Torsional and Bending Endurance Analysis of Screen-printed Interconnects on Various Flexible Substrates," in *2022 IEEE International Conference on Flexible and Printable Sensors and Systems (FLEPS)*, 10-13 July 2022 2022, pp. 1-4, doi: 10.1109/FLEPS53764.2022.9781508.

[15] D. Mitra *et al.*, "Conductive Electrifi and Nonconductive NinjaFlex Filaments based Flexible Microstrip Antenna for Changing Conformal Surface Applications," *Electronics*, vol. 10, no. 7, 2021, doi: 10.3390/electronics10070821.

[16] J. Lee, P. Lee, H. Lee, D. Lee, S. S. Lee, and S. H. Ko, "Very Long Ag Nanowire Synthesis and Its Application in a Highly Transparent, Conductive and Flexible Metal Electrode Touch Panel," *Nanoscale*, vol. 4, no. 20, pp. 6408-14, Oct 21 2012, doi: 10.1039/c2nr31254a.

[17] E. Altinozen, A. Vukovic, and P. Sewell, "Characterization of Flexible Interconnects," in *2022 Microwave Mediterranean Symposium (MMS)*, 9-13 May 2022 2022, pp. 1-4, doi: 10.1109/MMS55062.2022.9825602.

[18] X. Huang, T. Leng, K. H. Chang, J. C. Chen, K. S. Novoselov, and Z. Hu, "Graphene Radio Frequency and Microwave Passive Components for Low Cost Wearable Electronics," *2D Materials*, vol. 3, no. 2, 2016, doi: 10.1088/2053-1583/3/2/025021.

[19] E. Altinozen, I. Harrison, A. Vukovic, and P. Sewell, "Systematic generation of arbitrary antenna geometries," *IEEE Transactions on Antennas and Propagation*, 2021. [Online]. Available: https://nottingham-repository.worktribe.com/output/7022934.

[20] Y. Lipman, D. Levin, and D. Cohen-Or, "Green Coordinates," *ACM Trans. Graph.*, vol. 27, no. 3, pp. 1-10, 2008, doi: 10.1145/1360612.1360677.

[21] Y. Lipman and D. Levin, "Derivation and Analysis of Green Coordinates," *Computational Methods and Function Theory*, journal article vol. 10, no. 1, pp. 167-188, June 01 2010, doi: 10.1007/bf03321761.

[22] C. Christopoulos, *The Transmission-Line Modeling Method: TLM*. John Wiley & Sons, 1995.

[23] P. Sewell, J. G. Wykes, T. M. Benson, C. Christopoulos, D. W. P. Thomas, and A. Vukovic, "Transmission-line Modeling Using Unstructured Triangular Meshes," *IEEE Transactions on Microwave Theory and Techniques*, vol. 52, no. 5, pp. 1490-1497, 2004, doi: 10.1109/TMTT.2004.827027.

[24] P. Sewell, T. M. Benson, C. Christopoulos, D. W. P. Thomas, A. Vukovic, and J. G. Wykes, "Transmission-line Modeling (TLM) Based upon Unstructured Tetrahedral Meshes," *IEEE Transactions on Microwave Theory and Techniques*, vol. 53, no. 6, pp. 1919-1928, 2005, doi: 10.1109/tmtt.2005.848078.

[25] P. D. Sewell, T. M. Benson, C. Christopoulos, D. W. P. Thomas, A. Vukovic, and J. G. Wykes, "Implicit Element Clustering for Tetrahedral Transmission-Line Modeling (TLM)," *IEEE Transactions on Microwave Theory and Techniques*, vol. 57, no. 8, pp. 2005-2014, 2009, doi: 10.1109/tmtt.2009.2025451.

[26] X. Meng, P. Sewell, S. Phang, A. Vukovic, and T. M. Benson, "Modeling Curved Carbon Fiber Composite (CFC) Structures in the Transmission-Line Modeling (TLM) Method," *IEEE Transactions on Electromagnetic Compatibility*, vol. 57, no. 3, pp. 384-390, 2015, doi: 10.1109/temc.2015.2400055.

[27] A. Taflove, *Computational electrodynamics : the finite-difference time-domain method / Allen Taflove, Susan C. Hagness*, 3rd ed. ed. Boston [Mass.] London: Boston Mass. London : Artech House, 2005.

[28] X. Meng, P. Sewell, N. H. Rahman, A. Vukovic, and T. M. Benson, "Experimental Benchmarking of Unstructured Transmission-line Modelling (UTLM) Method in Modelling Twisted Wires," *ACES Express Journal*, vol. 1, no. 3, 2016.

[29] C. Jones, P. Sewell, T. M. Benson, A. Vukovic, X. Meng, and H. Bucklow, "Advanced Computational Electromagnetics at BAE Systems," 2016.

[30] S. Microwave, "The Design & Test of Broadband Launches up to 50 GHz on Thin & Thick Substrates," 2011. [Online]. Available: https://www.hasco-inc.com/content/Technical_Articles/Design_and_Test_Broadband_Launches.pdf

[31] D. M. Pozar, *Microwave Engineering*, 4th ed. Hoboken, N.J. : Wiley, 2012.

[32] GGIEMR. "George Green Institute for Electromagnetics Research." https://www.nottingham.ac.uk/research/groups/ggiemr/our-research/large-scale-electromagnetic-modelling/utlm-unstructured-transmission-line-modelling.aspx (accessed 2021).

Ekrem Altinozen currently pursuing a Ph.D. degree in electrical and electronic engineering from The University of Nottingham, Nottingham, U.K., His current research interests are conformal, wearable and foldable antennas and interconnects.

Ana Vukovic (M'97) was born in Nis, Serbia, in 1968. She received the Diploma of Engineering degree in electronics and telecommunications from the University of Nis, Nis, Yugoslavia, in 1992, and the Ph.D. degree from the University of Nottingham, Nottingham, U.K., in 2000. From 1992 to 2001, she was a Research Associate with the University of Nottingham. In 2001, she joined the School of Electrical and Electronic Engineering, University of Nottingham, as a Lecturer. In 2019 she became a Professor of electromagnetics applications. Her research interests are electromagnetics with a particular emphasis on applications in optoelectronics, microwaves, and EMC. Her research interests are electromagnetics with a particular emphasis on applications in optoelectronics, microwaves, and EMC.

Phillip Sewell (M'89-SM'04) was born in London, U.K., in 1965. He received the B.Sc. degree in electrical and electronic engineering (with first-class honors) and Ph.D. degree from the University of Bath, Bath, U.K., in 1988 and 1991, respectively. From 1991 to 1993, he was a Post-Doctoral Fellow with the University of Ancona, Ancona, Italy. In 1993, he became a Lecturer with the School of Electrical and Electronic Engineering, University of Nottingham, Nottingham, U.K. In 2001 and 2005, he became a Reader and Professor of electromagnetics at the University of Nottingham. His research interests involve analytical and numerical modeling of electromagnetic problems with application to opto-electronics, microwaves and aerospace applications.